Enhancement of the Strength of Biocomposite Films *via* Graphene Oxide Modification

Sijie Wang, Gang Liu, and Junwen Pu *

Chitosan-cellulose film is found in food processing and biotechnology because of its biocompatibility, biodegradability, and antibacterial property. Despite the excellent properties, the presence of intramolecular and intermolecular hydrogen bonds cause cellulose and chitosan to be insoluble in common solvents, resulting in limited mechanical strength. Graphene oxide has heavy oxygen-containing functional groups with excellent mechanical properties, which makes it an ideal filler for reinforcing polymers. In this work, blends of graphene oxide and chitosan-cellulose were successfully produced using 1-ally-3-methylimidazolium chloride ([Amim]Cl) and dimethyl sulfoxide (DMSO) as solvent media. Films were prepared by phase-transfer method and investigated by Fourier transform infrared analysis, scanning electron microscopy, atomic force microscopy, X-ray diffraction, thermogravimetric analysis, and mechanical tests. The absence of the bands corresponding to C=O stretching in graphene oxide and the -NH bending of amides and amines in chitosan, the absence of the diffraction peak at 2θ =11.3° in graphene oxide (XRD), and the improvement of thermal stability and mechanical property provided evidence for the interaction between graphene oxide and chitosan-cellulose.

Keywords: Cellulose; Chitosan; Graphene oxide; Blend

*Contact information: MOE Engineering Research Center of Forestry Biomass Materials and Bioenergy, Beijing Forestry University, Beijing, 100083, PR China; *Corresponding author: jwpu@bjfu.edu.cn*

INTRODUCTION

Cellulose, an abundant renewable natural material, is a polysaccharide composed of D-anhydroglucopyranose units joined by β-(1,4)-glycosidic bonds. Cellulose is used in many applications because of its low production cost, high porosity, film forming ability, high permittivity, and good chemical stability (Cherian *et al.* 2011; Singha and Thakur 2009). Nowadays, natural fibrous materials have become an alternative to traditional synthetic fibers (Singha and Thakur 2008; Thakur *et al*. 2013). Nevertheless, regenerated cellulose has poor mechanical properties, which restricts its applications with respect to membrane material. Therefore, incorporating other materials into cellulose is frequently used to obtain new materials with high chemical and physical properties.

Chitosan (CS), a natural biopolymer derived from plant cell wall and crustaceans, is the product of deacetylated chitin. It is widely applied on chemical, biochemical, and food processing due to their biocompatibility, biodegradability, and antibacterial properties (Fang *et al*. 2010). It also acts as an enhancer for papermaking because of its high density of amino and hydroxyl groups. However, cellulose and chitosan contain intramolecular and intermolecular hydrogen bonds that make them insoluble in common solvents, resulting in limited mechanical strength. Ionic liquids (ILs) are alternatives to traditional volatile solvents for dissolving cellulose (Gupta and Jiang 2015). In addition, studies reported that

the solvation effect of the aprotic co-solvent dimethyl sulfoxide broke down the ionic association of ILs and sped up the reaction rate (Yan *et al*. 2005). Owing to the similar molecular structure of chitosan and cellulose, high miscibility biocomposite films can be prepared. Shih *et al*. (2009) prepared cellulose-chitosan films using N-methylmorpholine-N-oxide as a solvent. The results indicated that blended films were not well miscible and rough with chitosan concentrations greater than 5 wt%. Stefanescu *et al*. (2009) employed ionic liquids as a solvent to dissolve chitosan and cellulose. High molecular weight chitosan is not soluble in ionic liquids; it only leads to swelling. Thus, the performance of the biocomposite membrane needs improvement by further modification.

The dispersion of nanoparticles in a polymer matrix may improve its mechanical, thermal, and/or electrochemical properties. Each nanoparticle improves one or more properties of a polymer matrix, including graphene oxide. Graphene, a 2-dimensional sheet of sp^2 bonded carbon, has distinctive optical, electrochemical, mechanical, and thermal properties (Nair *et al*. 2008; Yu *et al*. 2008). In contrast to graphene, graphene oxide (GO), a precursor of graphene prepared by chemical method, is heavily oxygenated with hydroxyl and epoxide functional groups located at the basal planes, in addition to carbonyl and carboxyl groups aimed at the sheet edges (Wang 2012). Its properties are similar to that of graphene. However, graphene oxide becomes an unordered insulating material due to intercalate oxide functional groups breaking the conjugated structure of graphene. These groups improve the interfacial interaction between graphene oxide and substrate materials, which leads to the comprehensive increase of physical properties in composite materials (Stankovich *et al*. 2006). In addition, pristine graphene and graphene oxide nanosheets exert an antibacterial effect on *Escherichia coli* by inducing its inner and outer cell membranes to degrade and reducing its viability (Tu *et al*. 2013).

The main components of a battery are the current collector, cathode, anode, and separator. The separator is essential in the battery performance, as it electronically isolates anode and cathode while allowing ions transport between them during the charging and discharging processes (Arora and Zhang 2004). However, the traditional polyolefin separators shrink significantly, which can be attributed to elevated temperature, causing the battery internal short circuit owing to their inferior surface energy and low melting point (Yong *et al*. 2016). Our interest is in obtaining electrochemical films used as battery separator from blends of graphene oxide, chitosan, and cellulose created by the presence of graphene oxide that has distinctive electrochemical and mechanical properties. More recently, studies have shown that mechanical stability of the separator is first question in battery aging (Peabody and Arnold 2011; Cannarella and Arnold 2013). Thus, 1-ally-3-methylimidazolium chloride ([Amim]Cl) and dimethyl sulfoxide (DMSO) were utilized to dissolve cellulose and chitosan. Graphene oxide was added to the cellulose-chitosan casting solution. The cellulose-chitosan material and the addition of graphene oxide material were compared and used to prepare films. Films were prepared by the phase-transfer method. Furthermore, the morphologies and mechanical properties of these membranes were studied.

EXPERIMENTAL

Materials

The cellulose pulp in this work was provided by the Senbo (Shandong, China) with a degree of polymerization (DP) of 650. Graphene oxide (GO) was supplied by Carbon

Century (Beijing, China). 1-Allyl-3-methylimidazolium chloride ([Amim]Cl) from Aichun (Shanghai, China) was purchased and used without further purification. Dimethyl sulfoxide (DMSO) and chitosan were obtained from commercial corporations and were analytical grade.

Preparation of Blended Membranes

The cellulose pulp was oven-dried under vacuum at 80 °C to remove water. The 5 wt% chitosan and known amounts (0%, 1%) of GO were ultrasonically dispersed in 10 g of a 7:3 (by mass) [Amim]Cl/DMSO mixture and made into a homogeneous slurry. DMSO was used to reduce the viscosity of IL. Subsequently, pulp (0.4 g) was slowly added to the mixed solvent while being stirred at 80 °C in a water bath for 30 min. To determine if cellulose particles were absolutely dissolved, a few drops of the mixture were checked under a polarized optical microscope. After completing each dissolution experiment, the mixture was poured onto a clean glass plate and transformed to a film with a thickness of 25 μm, using a scraper. The composite cellulose film was immersed and regenerated in a water bath overnight to ensure that the residual solvent was removed. Finally, the membrane was collected after being pressed and dried.

Table 1. Experimental Conditions

Sample ID	Reaction Conditions			
	[Amin]Cl/DMSO (g/g)	T (℃) Time (h)	CS (%)	GO (%)
S1	7:3	85;1	0	0
S2	7:3	85;1	5	0
S3	7:3	85;1	5	0.5
S4	7:3	85;1	5	1
S5	7:3	85;1	5	1.5

Fourier Transform Infrared (FT-IR) Analysis

FTIR spectra were obtained to confirm the chemical structure of the sample using a ThermoNicolet spectrometer (Madison, WI, USA). Its scan range was 4000 to 600 cm^{-1} at a resolution of 8 cm^{-1} in the transmission mode.

Scanning Electron Microscopy (SEM)

The morphology of the composite membranes was examined using a JEOL JSM-7001F scanning electron microscope (Tokyo, Japan). The samples were fractured in liquid nitrogen and sputtered with Au or Pt before being observed and photographed.

Atomic Force Microscopy (AFM)

The surface morphologies of the films were examined using a Bruker Multimode 8 atomic force microscope (Madison, WI, USA). RTESPA silica cantilevers were oscillated at a frequency of 300 KHz. Topographic (height) and phase images were obtained at 25 °C and 50% relative humidity.

Thermogravimetric Analysis (TGA)

Thermogravimetric analysis was performed on a TA Instruments SDT-Q600 thermobalance (New Castle, DE, USA). Each sample weighting approximately 8 mg was

heated from 50 °C to 600 °C with a rate of 10 °C/min under nitrogen. After being dried at 50 °C, the polymeric films were tested using TGA.

X-ray Diffraction (XRD) Measurements

A Shimadzu XRD-6000 diffractometer (Kyoto, Japan) was used for XRD analysis. The patterns were acquired with Cu Kα radiation over the diffraction angle (2θ) range of 5° to 40° at a scanning speed of 0.02°/min.

Mechanical Properties

The tensile strength and elongation at break (%) of composite films were measured with a Zwick/Roell-Z2.5 universal tensile tester (UIm, Germany) at a strain rate of 10 mm/min.

RESULTS AND DISCUSSION

Molecular Structure

The FT-IR spectra were used to examine the interactions between graphene oxide and chitosan-cellulose. The FT-IR spectra of the CS-GO-cellulose blends are presented in Fig. 1.

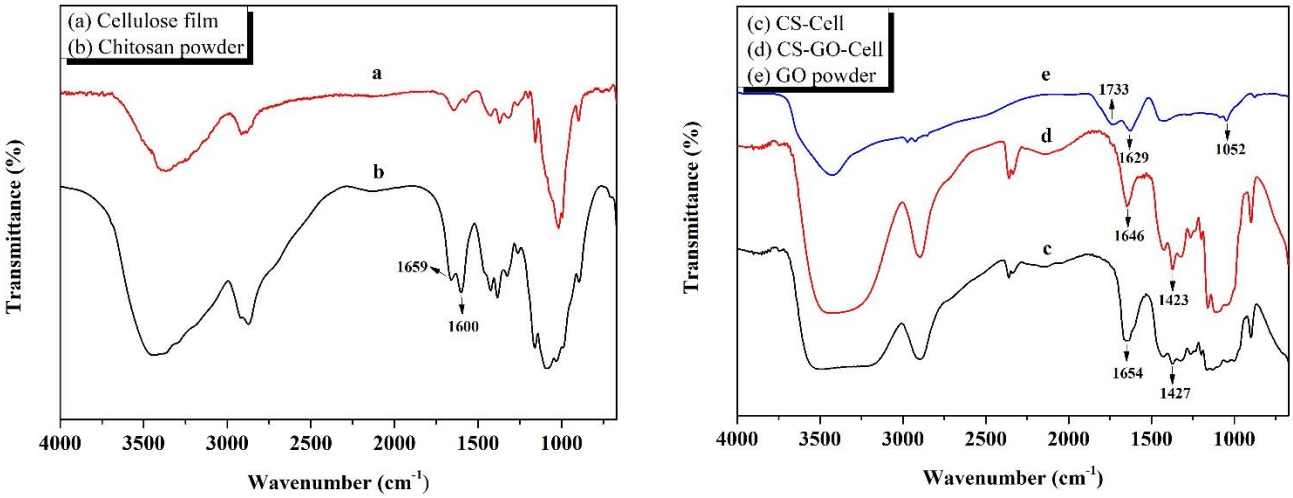

Fig. 1. FTIR spectra of chitosan (CS), cellulose film, graphene oxide (GO), chitosan-cellulose film (CS-Cell) and chitosan-graphene oxide-cellulose film (CS-GO-Cell)

The spectrum of chitosan powder showed similar bands to that of cellulose film except for the absorption band at 1600 cm^{-1}, which is a characteristic peak of -NH bending in amides and amines present in chitosan. The carbonyl stretch in the amides of chitosan appeared as a strong absorption at 1659 cm^{-1}. The presence of a lower frequency peak for the blends containing 5 wt% chitosan indicated the interaction between chitosan and cellulose in Fig. 1. The absorption of -NH bending was no longer observed in the spectra of the two polymeric films as a result of overlapping with the carbonyl stretch in amides, causing the band to shift to a higher frequency. This result is in agreement with previous results (Xu *et al.* 2005; Stefanescu *et al*. 2012). In the case of GO powder, the peaks at 3427 cm^{-1}, 1733 cm^{-1}, 1629 cm^{-1}, and 1052 cm^{-1} corresponded to O-H, C=O, C=C, and C-

O stretching vibrations, respectively (Marcano *et al*. 2010). Throughout the spectrum of the CS-GO-Cell film, intense peaks at 1733 cm^{-1} (the C=O stretching in GO powder) and at 1600 cm^{-1} (the -NH bending of amides and amines in CS powder) were all absent. The hydroxyl absorption peak shifted to lower frequency and higher relative intensity. These results could be ascribed to the synergistic effect of the hydrogen bond and the electrostatic interactions between chitosan and graphene oxide. Moreover, except for these, no significant changes were observed, indicating that GO physically dispersed in the CS-Cell film with the addition of GO.

Morphology of the Membranes

The SEM micrographs obtained from CS-Cell film and CS-GO-Cell film are presented in Figs. 2a and 2b. In the film with 5/95% chitosan-cellulose, the surface structure was homogeneous except for voids with no particular order, suggesting that the two polymers have good compatibility in Fig. 2a. This result may be explained by the same basic skeleton of the two polymers, and the interaction between the amino groups in the chitosan and hydroxyl groups in the cellulose as confirmed by the FT-IR spectrum. A structure with no phase separation of graphene oxide and chitosan-cellulose was observed in Fig. 2b. This result illustrates that the hydrogen bond and the electrostatic interactions enhanced miscibility between graphene oxide and chitosan-cellulose.

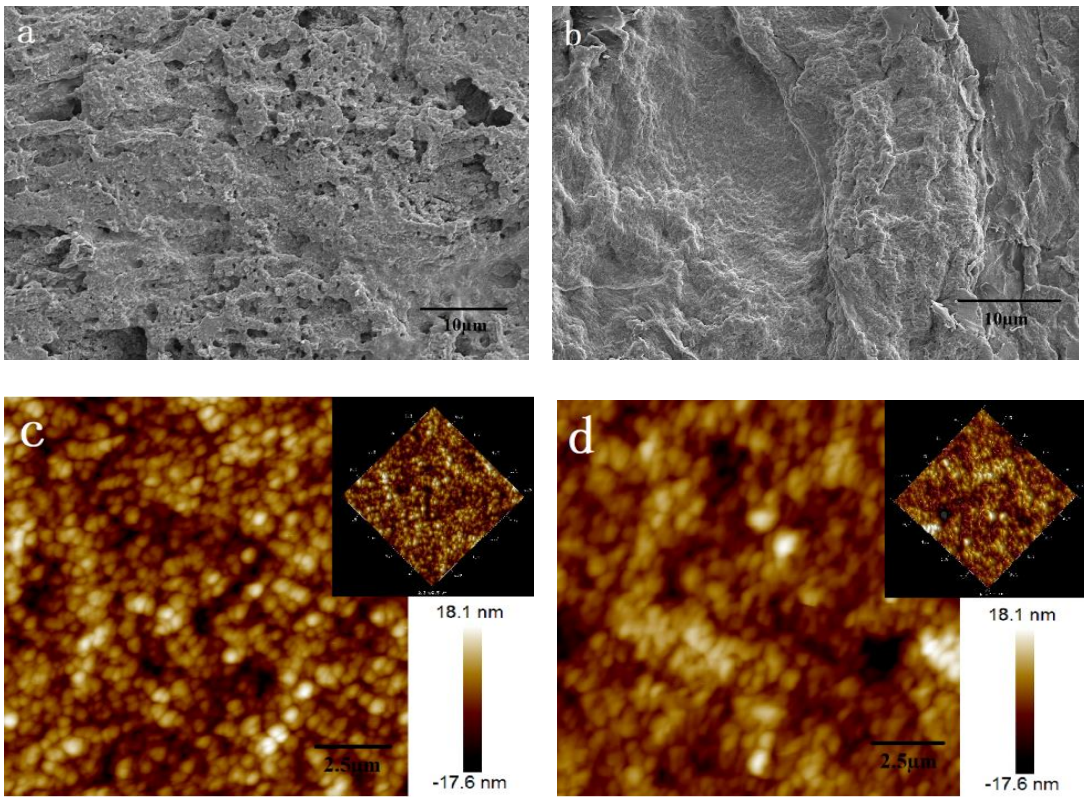

Fig. 2. SEM images of (a) CS-Cell film, and (b) CS-GO-Cell film. Insets are the respectively magnified images with scale bar of 1 0μm. AFM height images of (c) CS-Cell film, and (d) CS-GO-Cell film. Two scan sizes are shown: 2.5 × 2.5 μm.

To evaluate the surface topographies of the films, the height images were distinctly presented in the 3D AFM images in Figs. 2c and 2d. The roughness of films were obtained

by AFM analysis using the NanoScope Analysis software. The AFM image of 1% GO loading film revealed a porous thin film consisting of numerous tangled rods similar to that of the CS-Cell film. However, the root-mean-squared roughness of CS-Cell film was higher than that of 1% GO loading film, while lower average relative height. This effect could be attributed to partial flocculation of graphene oxide and chitosan because of electrostatic interactions.

Crystallite Structure

XRD spectroscopy was employed to unravel the change of blend membranes crystallinity due to the addition of graphene oxide. The diffraction of the cellulose film exhibited a peak at $2\theta = 19.9°$, which was consistent with cellulose II. Two main diffraction peaks of pure chitosan at the 2θ angle of 10.3° and 19.8° are shown in Fig. 3. When the two polymers were mixed at a chitosan to cellulose weight percent ratio of 5/95%, one diffraction peak with low intensity was observed at 2θ angles around 20°. The diffraction maxima at 2θ =10.3° of chitosan disappeared when they blended. The presence of results indicated that the formation of hydrogen bonds between chitosan and cellulose suppressed chitosan crystallization (Luo *et al*. 2008). As shown in Fig. 3, the pure GO power was in a crystalline state as indicated by the one main diffraction peak at the 2θ angle of 11.3°. The XRD pattern of the 1 wt% GO-coated film displayed the same as the chitosan-cellulose blend, with characteristic diffraction peaks at $2\theta = 20.1°$. The characteristic diffraction peak of graphene oxide was absent. Crystallinity index values of the CS-Cell film and the CS-GO-Cell film were 47.1% and 43.7%, respectively. Compared with the CS-Cell film, the decrease in crystallinity of 1% GO loading could be explained by the formation of hydrogen bonds between graphene oxide and chitosan-cellulose, disturbing the original structure of chitosan-cellulose because of the addition of graphene oxide. This result is in agreement with observations from the FT-IR analysis.

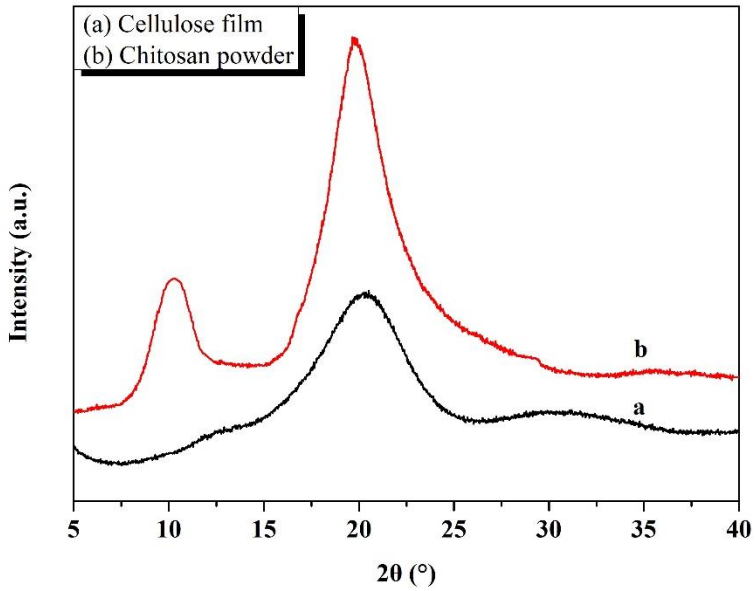

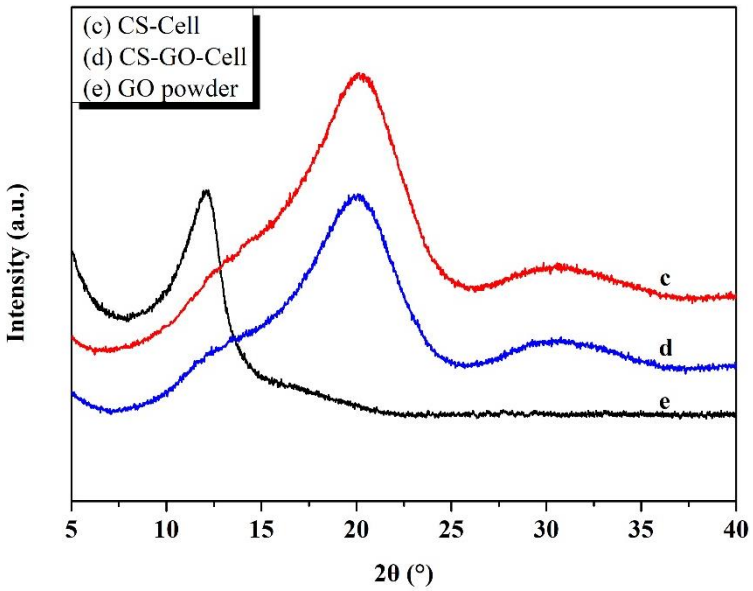

Fig. 3 XRD spectra of chitosan (CS), cellulose film, graphene oxide (GO), chitosan-cellulose film (CS-Cell) and chitosan-graphene oxide-cellulose film (CS-GO-Cell)

Thermal Stability

TGA/DTG analysis of incorporation of chitosan in cellulose film and CS-GO-Cell film is shown in Fig. 4. Both CS-Cell film and CS-GO-Cell film followed two stage degradation processes. The first weight loss stage was related to the water evaporation at approximately 100 ℃. During the second weight loss stage, the degradation temperature (T_{onset}) of the CS-GO-Cell film was similar to the value determined for the CS-Cell film, at approximately 250 °C, while the maximum decomposition temperature (T_{max}) of the two films were 331 °C and 334 °C, respectively.

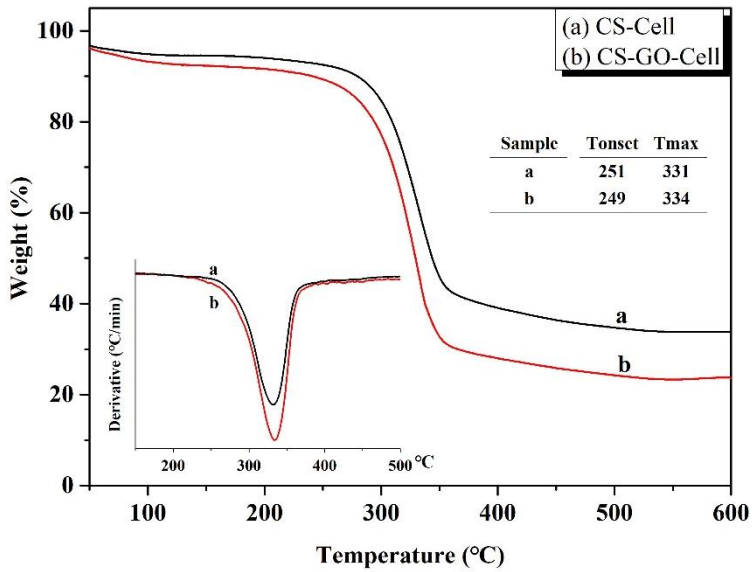

Fig. 4 TGA/DTG scans of chitosan-cellulose film (CS-Cell) and chitosan-graphene oxide-cellulose film (CS-GO-Cell)

The DTG degradation profiles of the two films displayed only one peak, with the peak of CS-GO-Cell film slightly shifted to a higher temperature. This change may be

related to an interaction between chitosan-cellulose and GO that impacted the degradation temperature of each component. A slight improvement was attributed to the hydrogen bonds and electrostatic adsorption between graphene oxide and the polymer that contribute to a uniform matrix with enhanced properties (Feng *et al*. 2012). Moreover, the reinforcing effect of graphene oxide reducing the chain segmental mobility is another factor. Thus, the thermal stability of modified film was better than that of CS-Cell film. However, it is worth noting that the increased weight loss of the CS-GO-Cell film depends on removing oxygen-containing functional groups of graphene oxide.

Mechanical Properties

The values measured for tensile properties of different polymeric films were derived and are found in Table 2. It was expected that incorporation of chitosan in cellulose film would enhance the mechanical properties of composite film, because of the interfacial adhesion. As shown in Table 2, the mechanical performance of CS-Cell film was increased compared with pure cellulose film. However, it was obvious that the trace amount of GO also had a remarkable effect on the mechanical behavior of CS-Cell film. The average tensile strength for CS-Cell film was 28.1 MPa. The strength was increased to 31.5 MPa for 0.5 % GO loading and further to 53.2 MPa for 1.5 wt%, which corresponds to an improvement of 89.1%. The average value of percentage elongation increased to 10.3% for 1% GO loading from 9.18% for the CS-Cell sample. These results could be explained by assuming that graphene oxide plays a role of a reticulation agent to improve the miscibility between cellulose and chitosan by hydrogen bonds (Miculescu *et al.* 2016). It is also worth mentioning the reinforcing effect of graphene oxide, leading to the enhancement in the tensile behavior of the composite film (Vadukumpully *et al.* 2011). However, a further increase in graphene oxide loading slightly increased the percentage elongation from 10.34% to 10.48%. It could be attributed to the restacking of graphene oxide exceeding the critical loading level (Vadukumpully *et al*. 2011). In view of higher mechanical properties for 1.5% GO loading, the electrochemical properties of the blended films need to be determined with respect to the application in battery separator in the future.

Table 2. Mechanical Properties of Different Films

Properties	Cellulose Film	CS-Cell Film	0.5% CS-GO-Cell Film	1% CS-GO-Cell Film	1.5% CS-GO-Cell Film
Tensile strength (MPa)	19.99	28.14	31.46	38.52	53.21
Breaking elongation (%)	6.59	9.18	9.57	10.34	10.48

CONCLUSIONS

1. Blends of graphene oxide (GO), chitosan (CS), and cellulose (Cell) were successfully prepared using [Amim]Cl/DMSO as a solvent *via* phase-transfer method. The CS-Cell film and CS-GO-Cell film were compared by FT-IR, SEM/AFM measurements, X-ray diffraction, TGA, and mechanical tests.

2. The absence of the C=O stretching in GO and the -NH bending of amides and amines in CS (FTIR), the decrease of crystallinity (XRD), and no apparent phase separator of three polymers (SEM) serve as evidence for the interaction among three polymers.
3. Thermal stability was found to be improved with addition of graphene oxide compared with CS-Cell film. Mechanical characterization of the CS-GO-Cell film demonstrated increase in tensile strength and breaking elongation with low graphene oxide loading. Moreover, the critical loading level of graphene oxide is crucial for its applications in composites.

ACKNOWLEDGMENTS

This work was sponsored by Special Fund for Beijing Common Construction Project and Beijing Forestry University, Grant No. 2016HXKFCLXY0015.

REFERENCES CITED

Arora, P., and Zhang, Z. (2004). "Battery separators," *Cheminform* 35(10), 4419-4462. DOI: 10.1002/chin.200450272

Cannarella, J., and Arnold, C. B. (2013). "Ion transport restriction in mechanically strained separator membranes," *Journal of Power Sources*, 226(226), 149-155. DOI: 10.1016/j.jpowsour.2012.10.093

Cherian, B. M., Leão, A. L., de Souza, S. F., Costa, L. M. M., de Olyveira G. M., Kottaisamy, M., Nagarajan, E. R., and Thomas, S. (2011). "Cellulose nanocomposites with nanofibres isolated from pineapple leaf fibers for medical applications," *Carbohydrate Polymers* 86(4), 1790-1798. DOI: 10.1016/j.carbpol.2011.07.009

Fang, M., Long, J., Zhao, W., Wang, L., and Chen, G. (2010). "pH-responsive chitosan-mediated graphene dispersions," *Langmuir* 26(22), 16771-16774. DOI: 10.1021/la102703b

Feng, Y., Zhang, X., Shen, Y., Yoshino, K., and Feng, W. (2012). "A mechanically strong, flexible and conductive film based on bacterial cellulose/graphene nanocomposite," *Carbohydrate Polymers* 87(1), 644-649. DOI: 10.1016/j.carbpol.2011.08.039

Gupta, K. M., and Jiang, J. (2015). "Cellulose dissolution and regeneration in ionic liquids: A computational perspective," *Chemical Engineering Science* 121, 180-189. DOI: 10.1016/j.ces.2014.07.025

Luo, K., Yin, J., Khutoryanskaya, O. V., and Khutoryanskiy, V. V. (2008). "Mucoadhesive and elastic films based on blends of chitosan and hydroxyethylcellulose," *Macromolecular Bioscience* 8(2), 184-192. DOI: 10.1002/mabi.200700185

Marcano, D. C., Kosynkin, D. V., Berlin, J. M., Sinitskii, A., Sun, Z., Slesarev, A., Alemany, L. B., Lu, W., and Tour, J. (2010). "Improved synthesis of graphene oxide," *ACS Nano* 4(8), 4806-4814. DOI: 10.1021/nn1006368

Miculescu, M., Thakur, V. K., Miculescu, F., and Voicu, S. I. (2016). "Graphene-based polymer nanocomposite membranes: A review," *Polymers for Advanced Technologies* 27(7), 844-859. DOI: 10.1002/pat.3751

Nair, R. R., Blake, P., Grigorenko, A. N., Novoselov, K. S., Booth, T. J., Stauber, T., Peres, N. M. R., and Geim, A. K. (2008). "Fine structure constant defines visual transparency of graphene," *Science* 320(5881), 1308-1308. DOI: 10.1126/science.1156965

Peabody, C., and Arnold, C. B. (2011). "The role of mechanically induced separator creep in lithium-ion battery capacity fade," *Journal of Power Sources* 196(19), 8147-8153. DOI: 10.1016/j.jpowsour.2011.05.023

Shih, C. M., Shieh, Y. T., and Twu, Y. K. (2009). "Preparation and characterization of cellulose/chitosan blend films," *Carbohydrate Polymers* 78(1), 169-174. DOI: 10.1016/j.carbpol.2009.04.031

Singha, A. S., and Thakur, V. K. (2008). "*Saccaharum cilliare* fiber reinforced polymer composites," *Journal of Chemistry* 5(4), 782-791.

Singha, A. S., and Thakur, V. K. (2009). "Synthesis, characterisation and analysis of *Hibiscus sabdariffa* fibre reinforced polymer matrix based composites," *Polymers & Polymer Composites* 17(3), 189-194.

Stankovich, S., Dikin, D. A., Dommett, G. H., Kohlhaas, K. M., Zimney, E. J., Stach, E. A., Piner, R. D., Nguyen, S. T., and Ruoff, R. S. (2006). "Graphene-based composite materials," *Nature* 442(7100), 282-286. DOI: 10.1038/nature04969

Stefanescu, C., Daly, W. H., and Negulescu, I. I. (2009). "Nucleophilic reactivity of chitosan in ionic liquids promoted by tert-amines," *Polymer Preprints* 15, 551-552.

Stefanescu, C., Daly, W. H., and Negulescu, I. I. (2012). "Biocomposite films prepared from ionic liquid solutions of chitosan and cellulose," *Carbohydrate Polymers* 87(1), 435-443. DOI: 10.1016/j.carbpol.2011.08.003

Thakur, V. K., Singha, A. S., and Thakur, M. K. (2013). "Fabrication and physico-chemical properties of high-performance pine needles/green polymer composites," *International Journal of Polymeric Materials & Polymeric Biomaterials* 62(4), 226-230. DOI: 10.1080/00914037.2011.641694

Tu, Y., Lv, M., Xiu, P., Huynh, T., Zhang, M., Castelli, M., Liu, Z., Huang, Q., Fan, C., Fang, H., and Zhou, R. (2013). "Destructive extraction of phospholipids from Escherichia coli membranes by graphene nanosheets," *Nature Nanotechnology* 8(8), 594-601. DOI: 10.1038/nnano.2013.125

Vadukumpully, S., Paul, J., Mahanta, N., and Valiyaveettil, S. (2011). "Flexible conductive graphene/poly(vinyl chloride) composite thin films with high mechanical strength and thermal stability," *Carbon* 49(1), 198-205. DOI: 10.1016/j.carbon.2010.09.004

Wang, S. Z. (2012). *Preparation and Functionalization of Oxidized Graphene*, Master's Thesis, Hefei University of Technology, Anhui, China.

Xu, Y. X., Kim, K. M., Hanna, M. A., and Nag, D. (2005). "Chitosan-starch composite film: Preparation and characterization," *Industrial Crops and Products* 21(2), 185-192. DOI: 10.1016/j.indcrop.2004.03.002

Yan, X., Sun, W., and Zhao, X. (2005). "Study on the solvent effect in acrylamide by NMR," *Chinese Journal of Magnetic Resonance* 22(4), 429-435.

Yong, X., Zou, H., Xiang, H, Xia, R., Liang, D., Shi, P., Dai, S., and Wang, H., (2016). "Enhancement on the wettability of lithium battery separator toward nonaqueous electrolytes," *Journal of Membrane Science* 503, 25-30. DOI: 10.1016/j.memsci.2015.12.025

Yu, A., Ramesh, P., Sun, X., Bekyarova, E., Itkis, M. E., and Haddon, R. C. (2008). "Enhanced thermal conductivity in a hybrid graphite nanoplatelet-carbon nanotube filler for epoxy composites," *Advanced Materials* 20(24), 4740-4744. DOI: 10.1002/adma.200800401

Article submitted: April 26, 2018; Peer review completed: June 28, 2018; Revised version received and accepted: July 2, 2018; Published: July 5, 2018.
DOI: 10.15376/biores.13.3.6321-6331